Proc. Natl. Acad. Sci. USA
Vol. 96, pp. 9409–9414, August 1999
Neurobiology

Inhibition of NF-κB potentiates amyloid β-mediated neuronal apoptosis

(IκB-α/tumor necrosis factor/oxidative stress/neuroprotection/preconditioning)

BARBARA KALTSCHMIDT*, MARTIN UHEREK*, HENNING WELLMANN*, BENEDIKT VOLK†, AND CHRISTIAN KALTSCHMIDT*‡

*Molecular Neurobiology Laboratory, Institute of Anatomy, Albert-Ludwigs-University, Stefan-Meier-Strasse 19, D-79104 Freiburg, Germany; and †Department of Neuropathology, Albert-Ludwigs-University, Breisacherstrasse 64, D-79106 Freiburg, Germany

Communicated by Dominick P. Purpura, Albert Einstein College of Medicine, Bronx, NY, June 4, 1999 (received for review January 4, 1999)

ABSTRACT **One mechanism leading to neurodegeneration during Alzheimer's disease (AD) is amyloid β peptide (Aβ) neurotoxicity. Aβ elicits in cultured central nervous system neurons a biphasic response: a low-dose neurotrophic response and a high-dose neurotoxic response. Previously we reported that NF-κB is activated by low doses of Aβ only. Here we show that NF-κB activation leads to neuroprotection. In primary neurons we found that a pretreatment with 0.1 μM Aβ-(1–40) protects against neuronal death induced with 10 μM Aβ-(1–40). As a known neuroprotective agent we next analyzed the effect of tumor necrosis factor α (TNF-α). Maximal activation of NF-κB was found with 2 ng/ml TNF-α. Pretreatment with TNF-α protected cerebellar granule cells from cell death induced by 10 μM Aβ-(1–40). This protection is described by an inverted U-shaped dose response and is maximal with a NF-κB-activating dose. The molecular specificity of this protective effect was analyzed by specific blockade of NF-κB activation. Overexpression of a transdominant negative IκB-α blocks NF-κB activation and potentiates Aβ-mediated neuronal apoptosis. Our findings show that activation of NF-κB is the underlying mechanism of the neuroprotective effect of low-dose Aβ and TNF-α. In accordance with these *in vitro* data we find that nuclear NF-κB immunoreactivity around various plaque stages of AD patients is reduced in comparison to age-matched controls. Taken together these data suggest that pharmacological NF-κB activation may be a useful approach in the treatment of AD and related neurodegenerative disorders.**

Alzheimer's disease (AD) is characterized by plaques within many brain regions, including the cerebellum (1). The major component of plaques is an amyloid peptide named βA4 or Aβ (2). Aβ is a proteolytic product of the larger amyloid precursor protein (APP; ref. 3). Further pathological criteria are the formation of neurofibrillary tangles (4) or increased advanced glycation end products (5), which also can activate NF-κB (6). Mutations in the presenilin genes 1 and 2 (for review see ref. 7) were described, which can lead to increased production of Aβ in transgenic mice (8). Mutant presenilin proteins interact directly with APP (9). Activation of NF-κB protects against the proapoptotic action of mutated presenilin-1 (10). Knockout of APP results in agenesis of corpus callosum, memory defects, and reactive gliosis (11, 12). An important mechanism leading to neurodegeneration during AD is Aβ neurotoxicity (13). Two dose-dependent effects of Aβ were described: a low neurotrophic dose and a high neurotoxic dose (13). Previously we reported that NF-κB is activated only by low doses of Aβ in cerebellar granule cells (14). Similarly Aβ could activate NF-κB in neuroblastoma cells (15), and Aβ-resistant cells have constitutive NF-κB activity (16).

To date five mammalian NF-κB DNA-binding subunits are known: p50, p52, p65 (RelA), c-Rel, and RelB (17). Inhibitory proteins are IκB-α, IκB-β, IκB-γ(p105), IκB-δ(p100), and IκB-ε (18, 19). Frequently NF-κB in the nervous system is composed from the DNA-binding subunits p50 and p65 (RelA) and an inhibitory subunit IκB-α (20). In neurons NF-κB can be activated either by glutamate (21, 22) or nerve growth factor (23) or is constitutively activated (24, 25). In glia it can be activated by various proinflammatory cytokines (20) or by nerve growth factor via $p75^{NTR}$ (26). Activation of NF-κB by external stimuli involves IκB kinases (for review see ref. 27), which are present in a large complex with the kinase Nemo (28), also called Ikkγ (29). This kinase complex is assembled with the help of the scaffold protein IKAP (30).

Expanding on our previous study (14), we have investigated here whether a preincubation with low amounts of Aβ leads to neuronal protection against a toxic dose of Aβ. We found that intracellular protection of neurons against neurotoxic stimuli is feasible and relies on activated NF-κB.

MATERIALS AND METHODS

Primary Culture. Primary rat cerebellar granule cells were prepared as described (31). Human recombinant tumor necrosis factor α (TNF-α) was from Boehringer-Mannheim. Aβ-(1–40) (lot nos. 506773 and 510598) and Aβ-(40–1) (lot no. H-2972) (Bachem) were used as described (14).

Immunofluorescence and Cell Survival Analysis. Cells were fixed for 2 min in ethanol and for 5 min in 3.7% formaldehyde and immunostained with an α-p65 mAb (Boehringer-Mannheim) detected with a biotinylated α-mouse antibody decorated with streptavidin Cy3. Analysis of neuronal survival in parallel to immunostaining was performed with the fluorescent nuclear dye 4′,6-diamidino-2-phenylindole (DAPI) (Boehringer-Mannheim), and images were digitally mounted (14) or digitally captured with a Princeton Instruments (Trenton, NJ) MicroMax camera. Nuclear chromatin morphology was analyzed with a 40× objective. Nonviable neurons were recognized by nuclear condensation and/or fragmented chromatin. The number of viable and nonviable neurons was counted in five fixed fields/chamber of up to five separate cultures.

Biolistic Transfection. One microgram DNA/1 mg Gold was used to coat 0.6-μm Gold particles (Bio-Rad) as described by the manufacturer. Granule cells were seeded in 4-well slides

The publication costs of this article were defrayed in part by page charge payment. This article must therefore be hereby marked "*advertisement*" in accordance with 18 U.S.C. §1734 solely to indicate this fact.

PNAS is available online at www.pnas.org.

Abbreviations: Aβ, amyloid β peptide; TNF-α, tumor necrosis factor α; AD, Alzheimer's disease; DAPI, 4′,6-diamidino-2-phenylindole; NBB, Netherlands Brain Bank; ROI, reactive oxygen intermediate; PDTC, pyrrolidine dithiocarbamate.

‡To whom reprint requests should be addressed. E-mail: kaltschm@ruf.uni-freiburg.de.

(Nunc) at a density of 500,000 cells/cm^2. Gold/shot (0.3 mg) was applied at 100 psi through a 100-μm nylonmesh with a Helios Gene Gun (Bio-Rad). For further details see ref. 62. LacZ staining together with IκB expression was done as described (32) with modifications. After LacZ staining the slides were washed and mounted with glycerin (90%) 1× PBS and 10 μg/ml DAPI (Boehringer Mannheim). Morphometric analysis was done by using IP-Lab-Spectrum software (Scanalytics, Fairfax, VA) on a Macintosh PowerPC. The minimal diameter of DAPI-stained nuclei was measured on at least five lacZ-expressing cells for each condition, with similar results from at least three independent experiments. Statistical analysis was done with ANOVA and Scheffé's *post hoc* test.

Histological Analysis. Isocortical tissue was obtained postmortem from patients with histopathologically confirmed AD and healthy controls. Frozen brain material from nondemented control ($n = 6$) and AD ($n = 11$) patients was obtained from the Netherlands Brain Bank (NBB) (coordinator, R. Ravid), nondemented control ($n = 3$) and AD ($n = 4$) patients from the National Neurological Research Specimen Bank, Los Angeles (director, W.W. Turtellotte) and nondemented control ($n = 6$) from the Medical Research Council Alzheimer's Disease Brain Bank, Department of Neuropathology, Institute of Psychiatry, London (coordinator: N.J. Cairns). All brains were neuropathologically investigated. The cases were matched for age, postmortem delay, and fixation duration. Eight-micrometer cryostat sections were cut from frozen tissue by using a Jung cryostat (Leica, Heidelberg, Germany) and mounted on gelatin-coated slides. Immunohistochemistry and mounting was performed essentially as described (14). Plaque types were classified on the morphology of thioflavin S fluorescence (33).

RESULTS

Preactivation of NF-κB After Aβ Treatment. Primary cerebellar granule cell cultures were used as a well-established culture system with a high content (>95%) of neurons. In these cultures 0.1 μM Aβ-(1–40) activates NF-κB, whereas the neurotoxic dose of 10 μM Aβ-(1–40) does not (14). Here we tested the physiological significance of this observation by using neurons pretreated with 0.1 μM Aβ-(1–40) for 24 h or left untreated. This preconditioning was followed by the addition of 10 μM Aβ-(1–40), which is significantly neurotoxic in this paradigm, for an additional 24 h. Cultures were tested for NF-κB activation with a mAb specific for the activated NF-κB p65 subunit (31) (Fig. 1*B*). Immunoreactivity with this antibody is detectable only after activation of NF-κB (14, 22, 26, 34). This type of single-cell analysis is superior when studying signal transduction in neuronal cultures (35, 36), because it can be limited to identified cell types. Furthermore neuronal cell death can be assayed with nuclear DAPI fluorescence (Fig. 1*B*) together with NF-κB activation. Cultures without pretreatment [0.1 μM Aβ-(1–40)] did not survive an insult with 10 μM Aβ-(1–40) for 24 h (Fig. 1*B*, *Left*), as apparent from the large number of pyknotic nuclei. In contrast, cultures pretreated with 0.1 μM Aβ-(1–40) survived very well after treatment (Fig. 1*B*, *Right*), as can be seen from the well-preserved nuclear structure. This survival effect correlates with a long-lasting activation of NF-κB p65 (Fig. 1*B*, *Right*). Quantitative analysis (Fig. 1*C*) showed a significant protection of neurons with activated NF-κB (92% alive) in comparison to neurons without pretreatment (38% alive), whereas a concentration of 0.1 μM Aβ is not neurotoxic (92% alive). The Aβ-induced NF-κB immunoreactivity is detected specifically by the anti-p65 mAb used here, because it could be blocked by preincubation with the peptide epitope used for generation of this antibody (Fig. 1*D*, Ab preabsorbed). Activation depends on the formation of reactive oxygen intermediates (ROIs), because it can be blocked by preincubation with

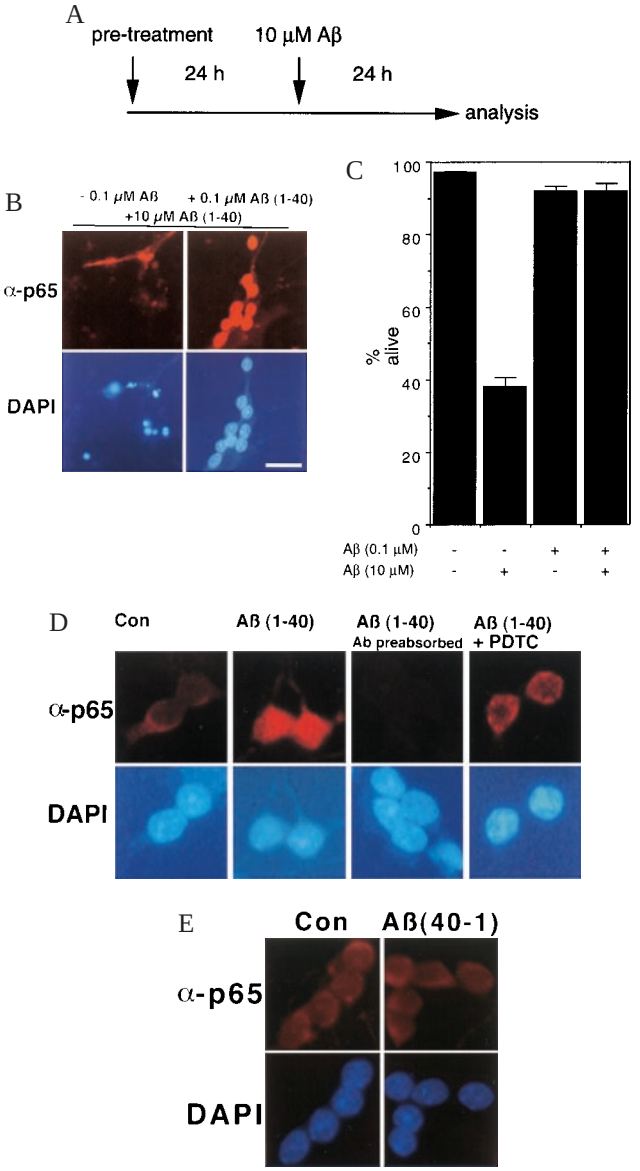

FIG. 1. Neuroprotection against Aβ is induced with low amounts of Aβ and depends on NF-κB activation. (*A*) Experimental setup for the treatment of primary cerebellar granule cells. Pretreatment was done with 0.1 μM of Aβ-(1–40), or mock 10 μM Aβ-(1–40) was used to induce cell death. (*B*) Granule cells were stained with anti-p65 NF-κB (*Upper*) and DAPI counterstaining (*Lower*). Neuronal death (see pyknotic nuclei) is induced after Aβ treatment without pretreatment (*Left*); long-lasting NF-κB activation is seen in neurons pretreated with Aβ (*Right*). Scale bar, 25 μm. (*C*) Quantification of neuronal cell death after Aβ treatment. Data are shown as mean ± SEM of five independent determinations. Treatment was as shown in *A*. Treatment with 10 μM of Aβ-(1–40) induced a > 60% reduction of viable cells ($P < 0.001$ to all other conditions), whereas pretreatment with 0.1 μM of Aβ-(1–40) reverses the neurotoxic effect. (*D*) Preincubation of the peptide epitope used for generation of the antibody totally abolished the p65 staining, showing the high specificity of the used anti-p65 antibody (compare second and third panels). A preincubation of 100 μM PDTC for 15 min blocks the activation of NF-κB by 0.1 μM Aβ (*Right*). (*E*) An Aβ with inversed sequence (Aβ-40–1) is not activating NF-κB in cerebellar granule cells.

100 μM of the antioxidant pyrrolidine dithiocarbamate (PDTC) (see Fig. 1*D*; compare *Left* and *Right*). As specificity control for the Aβ-induced NF-κB activation, a scrambled peptide was tested that did not activate NF-κB (see also ref. 2). In addition, an inverse Aβ (Aβ-40–1) did not induce any NF-κB response (Fig. 1*E*).

Preactivation of NF-κB After TNF-α Treatment. Here we asked whether TNF-α, another neuroprotective agent for hippocampal neurons (37), also can activate NF-κB in cerebellar granule cells. Optimal concentration of TNF-α for NF-κB activation was analyzed by indirect immunofluorescence. Unexpectedly we found a rather sharp concentration dependence with maximal NF-κB activation at a concentration of 2 ng TNF-α/ml (Fig. 2*A*). The activation of NF-κB at this concentration (Fig. 2*B*) is compatible with the previously reported TNF-α-mediated induction of κB binding activity in primary hippocampal neurons (38, 39). Because TNF-α at 4 ng/ml does not activate NF-κB, we wanted to use this observation as a pharmacological tool. Cerebellar granule cells were treated either with a NF-κB-activating dose of TNF-α (2 ng/ml) or with a nonactivating dose (4 ng/ml) by using a paradigm outlined in Fig. 1*A*. A pretreatment with 2 ng/ml for 24 h clearly protects against Aβ-induced neuronal death, whereas a pretreatment with 4 ng/ml does not (Fig. 2*B*). Quantification (Fig. 2*C*) showed that pretreatment with TNF-α alone does not affect neuronal survival. But only TNF-α at a concentration that activates NF-κB (2 ng/ml) is neuroprotective (Fig. 2*C*). Activation of NF-κB by TNF-α has a common denominator with the activation by Aβ, because both depend on the formation of ROIs and can be blocked by PDTC (see supplemental data on the PNAS web site, www.pnas.org). These data extend the findings of a neuroprotective role of TNF-α in hippocampal neurons (37) to a dose-dependent activation of NF-κB p65.

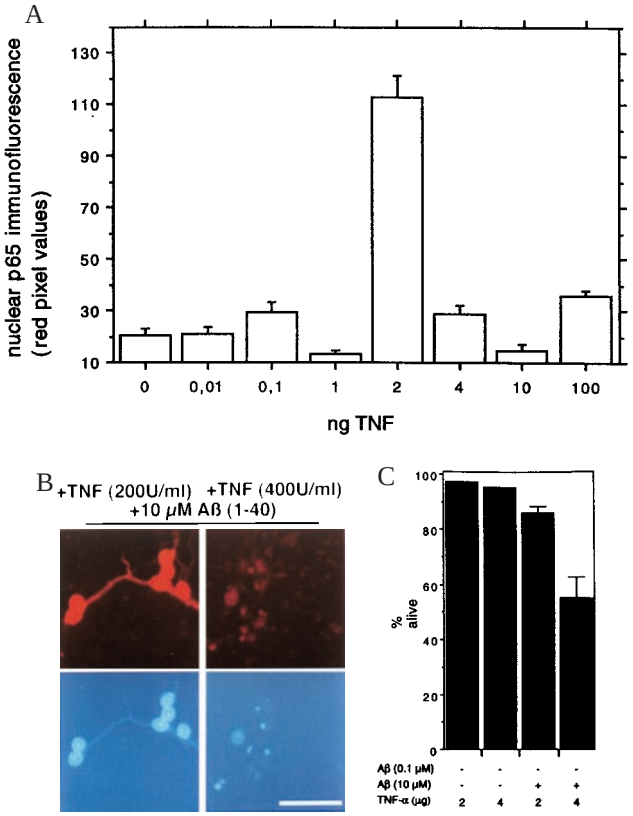

FIG. 2. TNF-α is activating NF-κB in granule cells. (*A*) Concentration dependence. Granule cells were left untreated (0) or incubated for 24 h with TNF-α at the concentrations indicated. The TNF-α-mediated increase in nuclear NF-κB p65 immunoreactivity is depicted as means ± SEM ($n > 10$ neurons). A treatment with 2 ng/ml TNF-α induces a long-lasting robust increase in nuclear NF-κB immunoreactivity ($P < 0.001$ to other concentrations). (*B*) Pretreatment with TNF-α effects survival of granule cells. Granule cells were pretreated with TNF-α at the concentrations indicated, (200 units/ml, which is 2 ng/ml, or 400 units/ml, which is 4 ng/ml) followed by additional 24-h incubation in the presence of 10 μM Aβ. Note: only the NF-κB-activating dose (2 ng/ml or 200 units/ml) leads to neuroprotection (*Left*). Cell cultures were analyzed by indirect immunofluorescence for an increase of α-p65 mAb immunoreactivity (*Upper*), and nuclear DAPI staining is shown below. Scale bar, 25 μm. (*C*) Quantification of neuronal cell death after Aβ treatment. Data are shown as mean ± SEM of five independent determinations. Treatment scheme was as shown in Fig. 1*A*. Treatment with 10 μM of Aβ-(1–40) after a pretreatment with 4 ng/ml TNF-α induced a > 40% reduction of viable cells ($P < 0.001$ to all other conditions), whereas pretreatment with 2 ng/ml TNF-α reverses the neurotoxic effect.

Interference with Neuroprotection via Overexpression of Transdominant Negative IκB-α. To further corroborate the pharmacological data, we wanted to specifically inhibit NF-κB, by using overexpression of a transdominant negative mutant (40) of IκB in cerebellar granule cells. This mutant is devoid of phosphorylation sites for IκB kinases (41), which transforms this molecule in a constitutive repressor. We used biolistic transfection to express either *Escherichia coli* β-galactosidase (LacZ) or LacZ together with transdominant negative IκB in cerebellar granule cells. These cells were treated with 0.1 μM Aβ-(1–40) to activate NF-κB, leading to neuroprotection, and stressed after 24 h with the toxic amount of Aβ for 3 h as shown in Fig. 3*A*. We used LacZ expression to identify transfected cells via blue staining with 5-bromo-4-chloro-3-indolyl β-D-galactoside (X-Gal) (see Fig. 3*B Upper*). LacZ-expressing cells depict a viable nuclear morphology (Fig. 3*B*, arrowheads), in comparison to surrounding nuclei of cells not expressing lacZ (Fig. 3*B Left*). In contrast, transfection of neurons with the IκB expression vector resulted in a high amount of cell death after the addition of 10 μM Aβ as apparent by the large amount of pyknotic cell nuclei (Fig. 3*B Right*, arrows). These pyknotic nuclei have a comparable greater diameter to those shown in Fig. 1*B*, because the analysis was done 3 h after treatment with 10 μM Aβ. Later on, after treatment all blue cells expressing IκB already were eliminated (data not shown), therefore 3 h

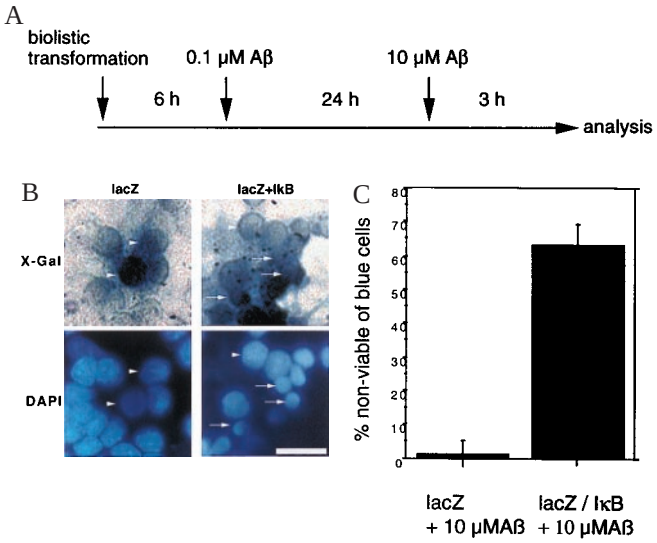

FIG. 3. Overexpression of IκB reverses the neuroprotective effect of pretreatment with a low dose of Aβ. (*A*) Experimental setup for the treatment and biolistic transfection of primary cerebellar granule cells. Primary granule cells were transfected with the expression vectors by the gene gun. After 6 h the cells were pretreated with 0.1 μM Aβ-(1–40) for 24 h to activate NF-κB, and after 3 h the survivors were counted. (*B*) Blow-up comparing transfection of LacZ alone (*Left*) or in combination with transdominant negative IκB expression vector (*Right*). (*Upper*) Staining of lacZ activity with 5-bromo-4-chloro-3-indolyl β-D-galactoside (X-Gal). (*Lower*) Nuclear DAPI stain. Note the shrinkage of nuclei after transfection with IκB (arrows), in contrast to viable cells (arrowheads), some dark blue cells after X-Gal stain show a somewhat reduced DAPI stain. (*C*) Quantification of cell death in LacZ-positive cells. Means (seven independent determinations) of dying cells were depicted ± SEM ($P < 0.001$). Scale bar, 25 μm.

of treatment was chosen for optimal analysis. Morphometric analysis of minimal nuclear diameter shows a mean diameter of 12.9 μm ± 0.09 (SEM) of lacZ-expressing cells (see Fig. 3*B Left*), whereas IκB-expressing cells show a shrunken pyknotic nucleus (Fig. 3*B Right*) with a mean diameter of 8.2 μm ± 0.2 ($P = 0.0024$). Occasionally the intensity of nuclear DAPI fluorescence (Fig. 3*B Lower*) is somewhat quenched in cells with a high level of X-Gal staining. By quantifying the number of blue cells with normal or shrunken pyknotic nucleus (Fig. 3*C*) a significant difference between the cells with or without IκB expression could be detected (Fig. 3*B*). In pretreated cultures transformed with a LacZ expression vector alone more than 80% survived the insult with 10 μM Aβ, whereas if the NF-κB activity was blocked via overexpression of a non-degradable transdominant negative IκB only about 30% of the transfected cells survived (Fig. 3*C*). These data point to a critical role of NF-κB in activating a gene expression program with neuroprotective function.

Analysis of Plaque Stages in AD Patients. Plaque types were classified on the morphology of the thioflavin S fluorescence as described (33): diffuse plaques, primitive plaques, classical plaques, and compacted plaques. This method might underrepresent the number of diffuse amyloid deposits, which are found more frequently with immunostaining methods (33). We analyzed the amount of each plaque type in AD patients and healthy controls. We found in the frozen material used here that the earliest plaque stage, the diffuse plaque, was most abundant (80%) in healthy controls (Fig. 4), whereas mature plaque types such as primitive, classical, and compact plaques were typical for AD patients (Fig. 4). This finding is in accordance with results obtained with the Bielschowsky silver-staining method (42). Primitive, classical, and compact types account for up to 70% of all plaques in disease patients. Taken together, a quantitative analysis of plaque types could distinguish between healthy (predominantly diffuse plaques) and AD patients (predominantly primitive and classical plaques).

Analysis of NF-κB Immunoreactivity Around Different Plaque Types. Based on this analysis we wanted to compare the nuclear NF-κB immunoreactivity around all plaque types in brain sections of healthy controls and AD patients. As reported earlier, NF-κB immunoreactivity is found predominantly in and around early plaque types of AD patients (14). Other reports described a generally higher NF-κB immunoreactivity in AD patients in comparison to controls (12, 43–45), but

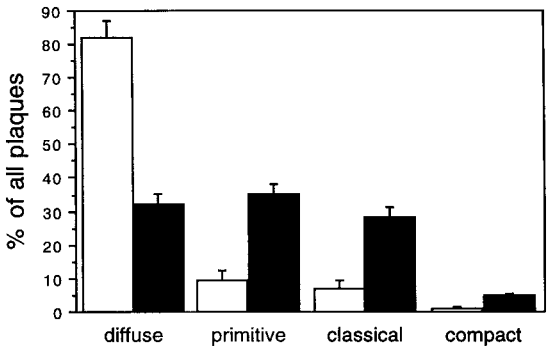

FIG. 4. Quantification of plaque types in AD patients and controls. Means ($n = 15$ for AD (89/220, 90/065, 90/077, 90/078, 90/080, 90/129, 90/139, 90/167, 90/174, 90/189, and 90/191 from NBB; 1956, 1998, 2195, and 2196 from Medical Research Council Alzheimer's Disease Brain Bank); ($n = 15$ for controls; 90/160, 90/206, 93/166, 93/204, 95/204, and 95/026 from NBB; 1933, 2296, and 2335 from the National Neurological Research Specimen Bank; 89/059, 89/072, 89/073, 89/084, 89/097, and 89/099 from Medical Research Council Alzheimer's Disease Brain Bank) expressing a percentage of the total plaque numbers in 98,175 mm^2 (five randomly selected microscopic views) were depicted.

increased neuronal immunoreactivity for p65 was predominantly cytoplasmatic (43). Here we are analyzing nuclear immunoreactivity in cells surrounding diffuse, primitive, and classical plaques of healthy controls (Fig. 5) and AD patients. Plaque types were analyzed by using thioflavin S staining on adjacent sections, but DAPI staining results in a rather similar staining of plaques (M.U., C.K., and B.K., unpublished observation, see Fig. 5). As an example we chose two different plaque types, primitive (Fig. 5 *a* and *c*) and classical (Fig. 5 *e* and *g*), from one representative AD patient (AD 90–129; NBB) and one age-matched control (93/166; NBB). In Fig. 5 *a*, *b*, *e*, and *f Left*, the strong nuclear NF-κB staining in cells surrounding the plaques of the control (see arrows) can be seen. Fig. 5 *c*, *d*, *g*, and *h Right* demonstrates the nuclear NF-κB staining in the AD patient (see arrows). In contrast to those of healthy controls, many of the cells surrounding plaques of AD patients show a vastly reduced NF-κB activity. Taken together data from 11 AD cases point to gradual loss of nuclear NF-κB immunoreactivity during plaque maturation (Table 1). In comparison to controls the NF-κB activity in cells around all plaque types is reduced at least 50% in AD patients.

DISCUSSION

This study shows that preactivation of NF-κB by low amounts of Aβ and TNF-α protects neurons through the activation of a NF-κB-dependent gene expression program. This effect can be blocked by overexpression of the specific NF-κB inhibitor IκB. Increased production of ROIs (e.g., H_2O_2) might activate NF-κB because the antioxidant PDTC can inhibit the Aβ-induced NF-κB activation. Also direct application of H_2O_2 (again in low amounts) can activate NF-κB in cerebellar granule cells (14). This effect of H_2O_2, as a crucial mediator for NF-κB activation, was described first for nonneuronal cells (46). Here we show that NF-κB activation via TNF-α in cerebellar granule cells follows an inverted U-shaped dose-response curve. A similar inverted U-shaped activation of NF-κB previously was described for Aβ and H_2O_2 (14). The reason for such a response could be the amount of ROI; a low amount of ROIs is activating NF-κB, whereas high amounts of ROIs inactivate the p65-subunit (see ref. 47 for discussion), because perinuclear aggregates are found with increased amounts of ROI-producing agents (14). In this line it was shown that a reduction of brain-derived κB-binding activity upon *in vitro* treatment with H_2O_2 could be restored by reducing thiols such as DTT or β-mercaptoethanol (48).

Taken together this activation of NF-κB leads to intracellular protection of cultured neurons against the neurotoxic action of large amounts of Aβs, using similar mechanisms as suggested by David Baltimore for intracellular immunization against viral infections (49).

Here we extend our previous finding of NF-κB immunoreactivity in and around plaques in AD patients (14) to a more detailed analysis. Although activated NF-κB is found in cells around all plaque types in both healthy and AD patients, here we describe a dramatic down-regulation of NF-κB activity from early to late plaque stages in AD patients. This difference might be one of the biochemical differences discriminating between healthy or diseased brains, which is important for AD (50). In this line it was shown that apoptotic cell death can be detected in AD (51) and that there is a progressive increase in cell death from early to late plaque stages (52). It is tempting to speculate that the inhibition of NF-κB observed here is the underlying mechanism for neuronal apoptosis as shown *in vitro* (see above) and for nonneuronal cells (53). We propose that NF-κB activation is necessary for the neurons to survive in the close vicinity of plaques. Because NF-κB activation is selectively lost around plaques of AD patients, this might be an important reason for the neurodegeneration observed around late plaque types, which are rare in healthy persons. We present

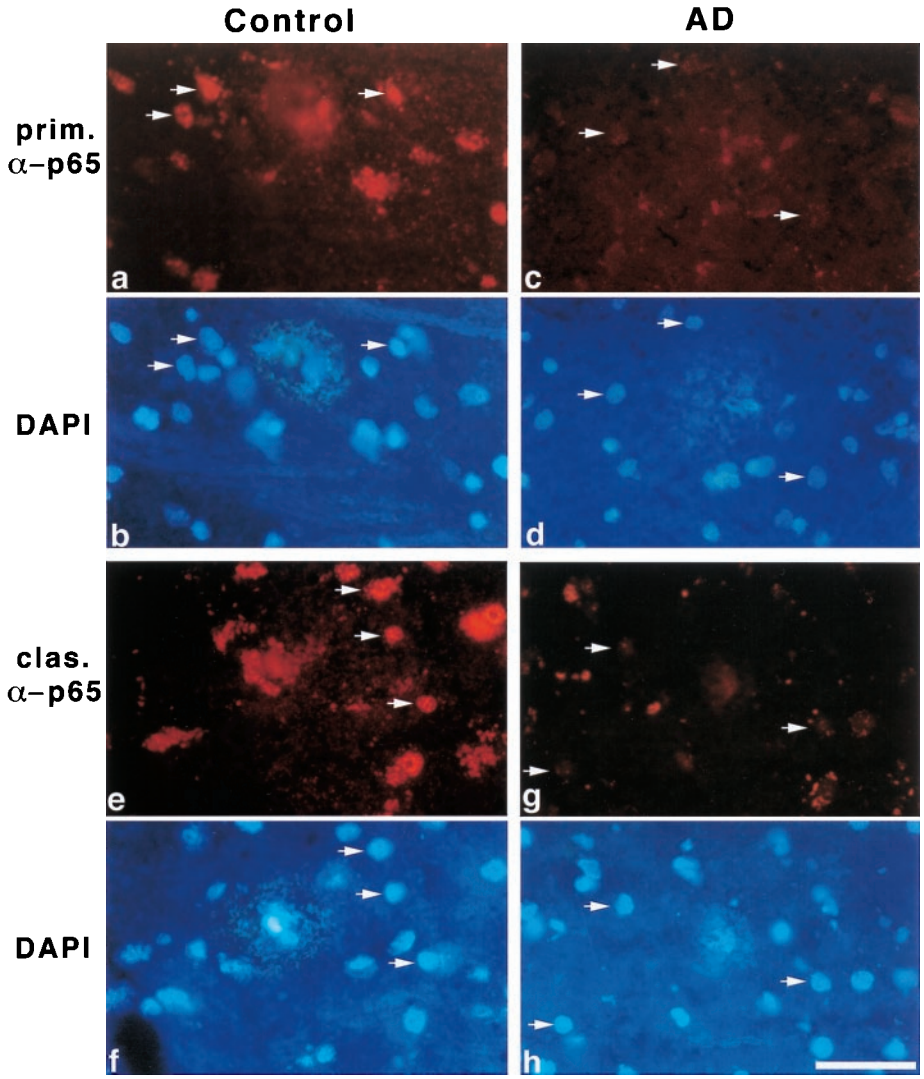

FIG. 5. Immunohistochemical analysis of nuclear NF-κB in cells around primitive (*a* and *c*) and classical plaques (*e* and *g*) of one representative AD patient (AD 90/129 from NBB and one representative age-matched control 93/166 from NBB), (*b*, *d*, *f*, and *g*) corresponding DAPI image of plaques. Note the reduced nuclear NF-κB immunoreactivity (compare arrows of *a* and *b* with arrows of *c* and *d* and arrows of *e* and *f* with the ones of *g* and *h*) in both plaque types of AD patients in comparison to healthy controls. Scale bar, 50 μm.

the hypothesis that reduced NF-κB activation in cells around plaques renders them sensitive to a neurotoxic insult by Aβ.

What can be the reason behind the reduction of NF-κB activation near plaques of AD patients? At least two scenarios might be envisaged: first, a direct inactivation of neuronal NF-κB caused by high amounts of Aβ in the plaque neighborhood, or second, an indirect inactivation via production of NF-κB-inhibiting substances by glial cells.

For the first scenario *in vitro* data from this study could support the following hypothesis about the role of NF-κB in neurons. The inverted U-shaped dose response for activation of NF-κB via Aβ suggest that higher doses and/or long exposure of neurons with Aβ could lead to an overload of oxidative stress (see ref. 47 for review), inactivating NF-κB-driven neuroprotective gene expression, and therefore might contribute directly to pathological mechanisms.

Table 1. Immunoreactivity for activated NF-kB, nuclear in cells around different plaque states

Diagnosis	Diffuse	Primitive	Classic	Compact
Nondemented Controls (n = 6)	58.5	34.6	19.4*	12.5*
AD (n = 11)	25.6	17.4	6.9	3.1

Immunoreactivity present in nuclei is expressed as a percentage of the total plaque number of patients and controls studied.
*Only rarely in nondemented controls.

For the second scenario glial cells can be envisaged as producers of disease-aggravating mediators. Reactive microglia frequently is found in or near plaques (54–57). Because astrocytes are absent is some plaques they do not seem to be directly involved in plaque formation (55). Activated microglia also is found in association of cerebellar plaques in AD (58) and might be crucially involved in the genesis of these plaques. Reactive microglia produces high amounts of proinflammatory cytokines such as TNF-α, IL-1β, and IL-6 or expressing MHC class II molecules as an activation marker (see ref. 59). Similarly, TNF-α production by microglia *in vitro* after Aβ stimulation (60) has been described together with a neurotoxic action of the stimulated microglia. This might very well resemble the *in vitro* effect described here of TNF-α-mediated NF-κB inhibition, which could result in a loss of neuroprotection. Thus inactivation of NF-κB around senile plaques also might be the consequence of high amounts of TNF-α produced directly by activated microglia in close vicinity to amyloid plaques (33). Directly linked with TNF-α production glial cells (e.g., microglia and astrocytes) could produce significant amounts of NO after proinflammatory stimulation. In this line

microglial production of NO can be stimulated via Aβ and IFN-γ treatment and depends on TNF-α production (60). NO might act in concert with TNF-α, because recently it was shown that NO produced in cultured astrocytes could effectively inhibit the activation of NF-κB (61). Taken together glia-produced TNF-α or NO might exert their local neurotoxicity via inactivation of neuronal NF-κB, abbrogating neuroprotective gene expression. Thus understanding the involvement of NF-κB in neurological diseases might open the route for the development of new classes of neuroprotective drugs modulating NF-κB activation.

We thank Dr. M. Frotscher for continuous support, A. Schulze-Specking and Elmar Böhm for superb technical assistance, and Dr. H. Stockinger for providing the monoclonal α-p65 antibody. Supply of tissue obtained from brain banks (see *Materials and Methods* and supplemental data at www.pnas.org) is gratefully acknowledged. This study was supported in part by the Volkswagen-Stiftung, Deutsche Forschungsgemeinschaft, and the European Community.

1. Selkoe, D. J. (1994) *Annu. Rev. Neurosci.* **17,** 489–517.
2. Masters, C. L., Simms, G., Weinman, N. A., Multhaup, G., McDonald, B. L. & Beyreuther, K. (1985) *Proc. Natl. Acad. Sci. USA* **82,** 4245–4249.
3. Kang, J., Lemaire, H. G., Unterbeck, A., Salbaum, J. M., Masters, C. L., Grzeschik, K. H., Multhaup, G., Beyreuther, K. & Muller, H. B. (1987) *Nature (London)* **325,** 733–736.
4. Braak, H. & Braak, E. (1997) *Neurobiol. Aging* **18,** 351–357.
5. Li, J. J., Dickson, D., Hof, P. R. & Vlassara, H. (1998) *Mol. Med.* **4,** 46–60.
6. Yan, S. D., Yan, S. F., Chen, X., Fu, J., Chen, M., Kuppusamy, P., Smith, M. A., Perry, G., Godman, G. C., Nawroth, P., *et al.* (1995) *Nat. Med.* **1,** 693–699.
7. Haass, C. (1997) *Neuron* **18,** 687–690.
8. Borchelt, D. R., Ratovitski, T., van Lare, J., Lee, M. K., Gonzales, V., Jenkins, N. A., Copeland, N. G., Price, D. L. & Sisodia, S. S. (1997) *Neuron* **19,** 939–945.
9. Weidemann, A., Paliga, K., Durrwang, U., Czech, C., Evin, G., Masters, C. L. & Beyreuther, K. (1997) *Nat. Med.* **3,** 328–332.
10. Guo, Q., Robinson, N. & Mattson, M. P. (1998) *J. Biol. Chem.* **273,** 12341–12351.
11. Müller, U., Cristina, N., Li, Z. W., Wolfer, D. P., Lipp, H. P., Rulicke, T., Brandner, S., Aguzzi, A. & Weissmann, C. (1994) *Cell* **79,** 755–765.
12. Zheng, H., Jiang, M., Trumbauer, M. E., Sirinathsinghji, D. J., Hopkins, R., Smith, D. W., Heavens, R. P., Dawson, G. R., Boyce, S., Conner, M. W., *et al.* (1995) *Cell* **81,** 525–531.
13. Yankner, B. A., Duffy, L. K. & Kirschner, D. A. (1990) *Science* **250,** 279–282.
14. Kaltschmidt, B., Uherek, M., Volk, B., Baeuerle, P. A. & Kaltschmidt, C. (1997) *Proc. Natl. Acad. Sci. USA* **94,** 2642–2647.
15. Behl, C., Davis, J. B., Lesley, R. & Schubert, D. (1994) *Cell* **77,** 817–827.
16. Lezoualc'h, F., Sagara, Y., Holsboer, F. & Behl, C. (1998) *J. Neurosci.* **18,** 3224- 3232.
17. Baldwin, A. J. (1996) *Annu. Rev. Immunol.* **14,** 649–683.
18. Whiteside, S. T. & Israël, A. (1997) *Semin. Cancer Biol.* **8,** 75–82.
19. Whiteside, S. T., Epinat, J. C., Rice, N. R. & Israel, A. (1997) *EMBO J.* **16,** 1413–1426.
20. O'Neill, L. A. J. & Kaltschmidt, C. (1997) *Trends Neurosci.* **20,** 252–258.
21. Guerrini, L., Blasi, F. & Denis, D. S. (1995) *Proc. Natl. Acad. Sci. USA* **92,** 9077–9081.
22. Kaltschmidt, C., Kaltschmidt, B. & Baeuerle, P. A. (1995) *Proc. Natl. Acad. Sci. USA* **92,** 9618–9622.
23. Wood, J. N. (1995) *Neurosci. Lett.* **192,** 41–44.
24. Kaltschmidt, C., Kaltschmidt, B., Neumann, H., Wekerle, H. & Baeuerle, P. A. (1994) *Mol. Cell. Biol.* **14,** 3981–3992.
25. Schmidt-Ullrich, R., Memet, S., Lilienbaum, A., Feuillard, J., Raphael, M. & Israël, A. (1996) *Development (Cambridge, U.K.)* **122,** 2117–2128.
26. Carter, B. D., Kaltschmidt, C., Kaltschmidt, B., Offenhauser, N., Böhm-Matthaei, R., Baeuerle, P. A. & Barde, Y. A. (1996) *Science* **272,** 542–545.
27. Stancovski, I. & Baltimore, D. (1997) *Cell* **91,** 299–302.
28. Yamaoka, S., Courtois, G., Bessia, C., Whiteside, S. T., Weil, R., Agou, F., Kirk, H. E., Kay, R. J. & Israël, A. (1998) *Cell* **93,** 1231–1240.
29. Rothwarf, D. M., Zandi, E., Natoli, G. & Karin, M. (1998) *Nature (London)* **395,** 297–300.
30. Cohen, L., Henzel, W. J. & Baeuerle, P. A. (1998) *Nature (London)* **395,** 292–296.
31. Kaltschmidt, C., Kaltschmidt, B., Henkel, T., Stockinger, H. & Baeuerle, P. A. (1995) *Biol. Chem. Hoppe Seyler* **376,** 9–16.
32. Liu, Z. G., Hsu, H., Goeddel, D. V. & Karin, M. (1996) *Cell* **87,** 565–576.
33. Dickson, D. W. (1997) *J. Neuropathol. Exp. Neurol.* **56,** 321–339.
34. Bethea, J. R., Castro, M., Keane, R. W., Lee, T. T., Dietrich, W. D. & Yezierski, R. P. (1998) *J. Neurosci.* **18,** 3251–3260.
35. Tao, X., Finkbeiner, S., Arnold, D. B., Shaywitz, A. J. & Greenberg, M. E. (1998) *Neuron* **20,** 709–726.
36. Deisseroth, K., Heist, E. K. & Tsien, R. W. (1998) *Nature (London)* **392,** 198–202.
37. Cheng, B., Christakos, S. & Mattson, M. P. (1994) *Neuron* **12,** 139–153.
38. Barger, S. W. & Mattson, M. P. (1996) *Mol. Brain Res.* **40,** 116–126.
39. Mattson, M. P., Goodman, Y., Luo, H., Fu, W. & Furukawa, K. (1997) *J. Neurosci. Res.* **49,** 681–697.
40. Traenckner, E. B., Pahl, H. L., Henkel, T., Schmidt, K. N., Wilk, S. & Baeuerle, P. A. (1995) *EMBO J.* **14,** 2876–2883.
41. Regnier, C. H., Song, H. Y., Gao, X., Goeddel, D. V., Cao, Z. & Rothe, M. (1997) *Cell* **90,** 373–383.
42. Huell, M., Strauss, S., Volk, B., Berger, M. & Bauer, J. (1995) *Acta Neuropathol.* **89,** 544–551.
43. Terai, K., Matsuo, A., McGeer, E. G. & McGeer, P. L. (1996) *Brain. Res.* **739,** 343–349.
44. Kitamura, Y., Shimohama, S., Ota, T., Matsuoka, Y., Nomura, Y. & Taniguchi, T. (1997) *Neurosci. Lett.* **237,** 17–20.
45. Boissiere, F., Hunot, S., Faucheux, B., Duyckaerts, C., Hauw, J. J., Agid, Y. & Hirsch, E. C. (1997) *NeuroReport* **8,** 2849–2852.
46. Schreck, R., Rieber, P. & Baeuerle, P. A. (1991) *EMBO J.* **10,** 2247–2258.
47. Kaltschmidt, B., Sparna, T. & Kaltschmidt, C. (1999) *Antioxidants Redox Signaling*, in press.
48. Salminen, A., Liu, P. K. & Hsu, C. Y. (1995) *Biochem. Biophys. Res. Commun.* **212,** 939–944.
49. Baltimore, D. (1988) *Nature (London)* **335,** 395–396.
50. Dickson, D. W. (1997) *Neurobiol. Aging* **18,** 21–26.
51. Lassmann, H., Bancher, C., Breitschopf, H., Wegiel, J., Bobinski, M., Jellinger, K. & Wisniewski, H. M. (1995) *Acta Neuropathol.* **89,** 35–41.
52. Sheng, J. G., Zhou, X. Q., Mrak, R. E. & Griffin, W. S. (1998) *J. Neuropathol. Exp. Neurol.* **57,** 714–717.
53. Van Antwerp, D. J., Martin, S. J., Verma, I. M. & Green, D. R. (1998) *Trends Cell Biol.* **8,** 107–111.
54. McGeer, P. L., Itagaki, S., Tago, H. & McGeer, E. G. (1987) *Neurosci. Lett.* **79,** 195–200.
55. Dickson, D. W., Farlo, J., Davies, P., Crystal, H., Fuld, P. & Yen, S. H. (1988) *Am. J. Pathol.* **132,** 86–101.
56. Wisniewski, H. M., Wegiel, J., Wang, K. C., Kujawa, M. & Lach, B. (1989) *Can. J. Neurol. Sci.* **16,** 535–542.
57. Mattiace, L. A., Davies, P. & Dickson, D. W. (1990) *Am. J. Pathol.* **136,** 1101–1114.
58. Mattiace, L. A., Davies, P., Yen, S. H. & Dickson, D. W. (1990) *Acta Neuropathol.* **80,** 493–498.
59. Dickson, D. W., Lee, S. C., Mattiace, L. A., Yen, S. H. & Brosnan, C. (1993) *Glia* **7,** 75–83.
60. Meda, L., Cassatella, M. A., Szendrei, G. I., Otvos, L., Jr., Baron, P., Villalba, M., Ferrari, D. & Rossi, F. (1995) *Nature (London)* **374,** 647–650.
61. Togashi, H., Sasaki, M., Frohman, E., Taira, E., Ratan, R. R., Dawson, T. M. & Dawson, V. L. (1997) *Proc. Natl. Acad. Sci. USA* **94,** 2676–2680.
62. Wellmann, H., Kaltschmidt, B. & Kaltschmidt, C. (1999) *J. Neurosci. Methods*, in press.